Gas– Liquid Equilibrium Data for the Mixture Gas of Sulfur Dioxide/Nitrogen with Ethylene Glycol at Temperatures from (298.15 to 313.15) K under Low Pressures

5 AUTHORS, INCLUDING:

Jianbin Zhang

Peking University

47 PUBLICATIONS   **396** CITATIONS

Gas−Liquid Equilibrium Data for the Mixture Gas of Sulfur Dioxide/Nitrogen with Ethylene Glycol at Temperatures from (298.15 to 313.15) K under Low Pressures

Jianbin Zhang,[†] Pengyan Zhang,[‡] Guohua Chen,[‡] Fang Han,[‡] and Xionghui Wei*,[†]

Department of Applied Chemistry, College of Chemistry and Molecular Engineering, Peking University, Beijing 100871, China, and College of Chemical Engineering, Inner Mongolia University of Technology, Huhhot 010051, China

Isothermal gas−liquid equilibrium (GLE) data have been measured for the system SO_2 + N_2 + ethylene glycol (EG), respectively, at (298.15, 303.15, 308.15, and 313.15) K and SO_2 partial pressures in the range of (0 to 120) Pa. Measurements were carried out by a saturation method using a glass absorption apparatus, which were controlled at constant temperatures by a thermostatic circulation bath with a Beckmann thermometer. The GLE data were obtained with uncertainties within ± 0.02 K for temperature, ± 0.133 kPa for total pressure, ± 2.5 % for SO_2 concentration in the gas phase, and ± 0.6 % for SO_2 concentration in the liquid phase. The peculiarity of this work is used to provide important GLE data for the design and operation of the absorption and desorption process in flue gas desulfurization (FGD) with potential industrial application of the solutions containing EG.

Introduction

Sulfur dioxide (SO_2) is an important atmospheric pollutant in environmental protection. Its main source is flue gas from the burning of fuels with high sulfur content from 0.03 mg·m^{-3} in the air up to several g·m^{-3} in a typical flue gas.[1] Removal of SO_2 from flue gas is an increasingly important environmental challenge, on one hand, because of the lowering of the admissible emission limit and, on the other hand, due to the fact that numerous desulfurization processes, such as limestone scrubbing, produce a large volume of solid waste. There is a growing interest in the use of organic solvents for SO_2 removal, and organic solvents used as absorbents have been identified as an option among the regenerative process.[2–6] In these organic solvents, alcohols show the favorable absorption and desorption properties for acid gases in the factual industrial processes;[7] therefore, our research group has been paying great attention to the scrubbing technique by the alcohol−water system for several years.[8,9]

Ethylene glycol (EG) is an important industrial solvent, which may be used in the cleaning of exhaust air and gas streams from industrial production plants because of its favorable properties, such as low vapor pressure, low toxicity, low viscosity, high chemical stability, and low melting point. On the other hand, EG presents native hydrogen bonding sites for FGD so that the potential desorption characters are presented in the regenerative processes of desulfurizing solutions dissolving SO_2. Knowledge of the GLE data for dilute SO_2 (< 1000 ppmv, about 3000 mg·Nm^{-3}) with EG under low total pressures is an indispensable requirement for the design of absorption and desorption processes of desulfurizing solutions in FGD processes. But the GLE data are very lacking in the current equilibrium data, so we have to determine the GLE data for the system SO_2 + N_2

* To whom correspondence should be addressed. Tel.: +86-010-62751529. Fax: +86-010-62751529. E-mail: xhwei@pku.edu.cn.
[†] Peking University.
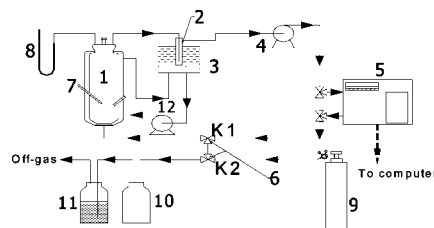[‡] Inner Mongolia University of Technology.

Figure 1. Sketch of the experimental apparatus: 1, jacketed vessel; 2, cold trap; 3, thermostatic bath; 4, gas circulatory pump; 5, GC; 6, regulating valve; 7, thermometer; 8, pressure meter; 9, SO_2/N_2 gas cylinder; 10, buffer; 11, absorption apparatus; 12, liquid circulatory pump.

+ EG for the future industrial application of the solutions containing EG.

The present work was mainly focused on providing a GLE measurement and presenting the GLE data for the system SO_2 + N_2 + EG in the temperature range from (298.15 to 313.15) K reported, respectively, at (298.15, 303.15, 308.15, and 313.15) K and SO_2 partial pressures in the range from (0 to 120) Pa.

Experimental Section

Materials. The certified standard mixtures (SO_2 + N_2), including 50.2 ppmv, 109 ppmv, 310 ppmv, 595 ppmv, 1010 ppmv, and 1970 ppmv (1970 ppmv mixture for the GLE experiments mainly), purchased from the Standard Things Center (China), were employed to determine the GLE data for the system SO_2 + N_2 + EG in this work. EG (≥ 99.4 %) was purified from EG (A.R. ≥ 98.0 %, made in China), dehydrated by Na_2SO_4, and refined by rectification. The purity of the final samples, as found by gas chromatograph, was better than 99.4 %.

Apparatus and Procedure. The experimental apparatus used in this work is shown in Figure 1. SO_2/N_2 mixtures from the gas cylinder (9) were poured into the apparatus through switching the regulating valve K1 and K2 (6) and were recycled

Table 1. Experimental Data of 1000 ppmv SO$_2$ by GC and Analyses of Data

certified SO$_2$ concentration	retention time/min	average retention time/min	uncertainty of retention time/%	peak area	average peak area	uncertainty of peak area/%
1000 ppmv	0.840605	0.84214	< ± 0.18	60919.88	60864.01	< ± 0.092
	0.840993			60893.37		
	0.84133			60895.8		
	0.8418			60861.56		
	0.84201			60858.68		
	0.84223			60860.18		
	0.84268			60852.32		
	0.84253			60856.98		
	0.84293			60842.94		
	0.84314			60823.64		
	0.84327			60838.77		

Table 2. Calibrating Relation for the FPD Detector

calibrating condition		calibrating relation: y = ax + b		calibrating condition		calibrating relation: y = ax + b	
T/K	p/10 Pa	a	b	T/K	p/10 Pa	a	b
298.15	10186	0.5750	−0.9764	303.15	10186	0.5533	−0.7649
	10719	0.5794	−1.0555		10719	0.5565	−0.7576
	11253	0.5712	−0.9888		11253	0.5502	−0.7886
	11785	0.5654	−0.9497		11785	0.5473	−0.7695
	12319	0.5637	−0.9932		12319	0.5546	−0.8937
	12853	0.5622	−1.0039		12853	0.5589	−0.9724
	13385	0.5667	−1.0783		13385	0.5577	−0.9969
	13919	0.5559	−0.9979		13919	0.5584	−1.0337
	14453	0.5511	−0.9667		14453	0.5589	−1.0672
	14986	0.5496	−0.9836		14986	0.5594	−1.0991
308.15	10186	0.5459	−0.6629	313.15	10186	0.5441	−0.6359
	10719	0.5472	−0.6580		10719	0.5520	−0.7595
	11253	0.5458	−0.6790		11253	0.5482	−0.7539
	11785	0.5462	−0.7295		11785	0.5564	−0.8565
	12319	0.5450	−0.7471		12319	0.5608	−0.9547
	12853	0.5394	−0.7255		12853	0.5534	−0.9095
	13385	0.5559	−0.9637		13385	0.5566	−1.0042
	13919	0.5555	−0.9949		13919	0.5544	−0.9853
	14453	0.5551	−1.0224		14453	0.5548	−1.0196
	14986	0.5545	−1.0482		14986	0.5552	−1.0526

Table 3. GLE Data for the SO$_2$ + N$_2$ + EG System at 298.15 K and 101.86 kPa

y_{SO_2} ppmv	C_{SO_2} mg·L^{-1}	p_{SO_2} Pa	y_{SO_2} ppmv	C_{SO_2} mg·L^{-1}	p_{SO_2} Pa
31.47	49.18	3.21	434.25	104.17	40.53
44.42	17.58	4.53	501.80	114.22	46.83
65.33	25.48	6.68	530.35	134.33	49.17
111.51	21.50	11.15	553.63	147.73	51.344
122.31	33.79	12.25	584.66	142.15	53.98
141.00	40.49	14.05	602.83	144.38	55.57
163.02	46.08	16.04	626.63	147.73	57.47
196.51	53.90	19.14	646.38	155.55	59.12
217.89	56.13	21.17	708.53	169.68	72.35
248.25	61.72	23.95	722.45	170.80	73.59
255.66	69.54	24.73	745.58	176.39	75.74
257.76	67.30	24.69	839.71	215.49	85.43
275.64	71.77	26.47	845.59	222.19	86.16
276.72	70.65	26.37	917.39	255.70	93.45
287.96	77.35	27.48	940.02	267.99	95.97
330.00	78.47	31.37	988.81	307.09	100.72
366.85	89.64	34.65	1005.61	318.26	102.58
404.84	92.9946	38.06	1043.41	343.95	106.56

Table 4. GLE Data for the SO$_2$ + N$_2$ + EG System at 298.15 K and 112.53 kPa

y_{SO_2} ppmv	C_{SO_2} mg·L^{-1}	p_{SO_2} Pa	y_{SO_2} ppmv	C_{SO_2} mg·L^{-1}	p_{SO_2} Pa
51.66	21.09	5.82	429.60	106.17	48.33
65.55	24.61	7.38	467.61	114.07	52.60
83.88	29.87	9.46	513.19	123.72	57.78
103.35	35.14	11.62	567.30	133.38	63.74
127.10	36.89	14.29	601.14	148.30	67.48
150.56	44.79	16.90	660.53	158.83	74.33
164.49	51.82	18.51	714.00	182.53	80.07
247.26	56.20	27.78	795.89	219.40	89.56
272.68	64.10	30.69	819.32	236.91	92.14
304.89	73.76	34.28	886.65	254.47	99.81
340.65	80.78	38.17	898.66	286.07	101.14
374.96	83.42	42.17	930.21	350.14	104.45
398.67	91.25	44.70	980.41	392.28	110.21

through a jacketed vessel (1), cold trap (2), and gas circulatory pump (4) for whole recycling process. Liquid temperatures were registered on a standard thermometer (7) at different points, and the temperatures do not vary more than 0.02 K. Total pressures were recorded on a pressure meter (8). SO$_2$ concentrations in the gas phase were determined by a GC (5) FPD detector. After GLE experiments were performed, the mixture gas was dis-

charged out by switching the regulating valve (6) and passing buffer (10) and absorption apparatus containing alkaline solution (11).

Experimental Procedure. Experiments were carried out, respectively, at (298.15, 303.15, 308.15, and 313.15) K kept at a constant temperature using a CS 501 thermostatted bath with a Beckmann thermometer purchased from Huanghua Meter Factory (Hebei province, China) with a precision of ± 0.02 K and inspected using an accurate thermometer purchased from Fuqiang Meter Factory (Hebei province, China) with the precision of ± 0.02 K and the total pressures of (101.86, 112.53, 123.19, 133.85, and 144.53) kPa inspected by a pressure gauge purchased from Fuqiang Meter Factory

Table 5. GLE Data for the SO_2 + N_2 + EG System at 298.15 K and 123.19 kPa

y_{SO_2}	C_{SO_2}	p_{SO_2}	y_{SO_2}	C_{SO_2}	p_{SO_2}
ppmv	mg·L^{-1}	Pa	ppmv	mg·L^{-1}	Pa
27.62	21.09	3.37	501.30	127.81	60.93
42.79	20.15	5.20	534.96	133.43	65.20
91.60	34.19	11.18	580.28	150.97	70.81
137.51	43.85	16.81	632.93	167.81	77.22
140.80	59.65	17.15	642.23	167.11	78.39
186.16	42.97	22.70	688.16	193.78	83.91
199.23	56.23	24.30	719.40	230.36	87.87
246.49	69.57	30.20	752.12	247.21	91.66
288.46	77.29	35.15	791.65	250.01	96.69
318.90	87.81	39.06	838.77	272.47	102.05
356.84	98.34	43.34	869.94	289.31	106.11
363.21	97.64	44.26	882.18	292.12	107.35
393.90	106.76	48.14	908.01	328.61	110.87
458.33	119.39	55.88	943.56	356.68	115.55

Table 6. GLE Data for the SO_2 + N_2 + EG System at 298.15 K and 133.85 kPa

y_{SO_2}	C_{SO_2}	p_{SO_2}	y_{SO_2}	C_{SO_2}	p_{SO_2}
ppmv	mg·L^{-1}	Pa	ppmv	mg·L^{-1}	Pa
40.30	21.09	5.34	592.82	157.86	77.93
73.43	28.04	9.64	607.10	163.48	79.84
97.03	32.25	12.76	661.69	190.15	87.42
157.02	46.28	20.60	676.17	197.83	88.96
162.08	49.09	21.46	701.52	196.29	92.50
207.44	63.83	27.12	755.25	229.68	99.90
279.22	77.86	36.70	793.45	270.03	104.68
309.97	86.29	40.68	824.59	283.94	109.09
355.40	99.62	46.65	861.71	300.64	114.56
406.76	112.25	53.40	890.60	321.51	117.68
473.07	126.29	62.34	906.66	343.77	119.72
515.17	134.00	67.93	912.99	345.16	120.42

Table 7. GLE Data for the SO_2 + N_2 + EG System at 298.15 K and 144.53 kPa

y_{SO_2}	C_{SO_2}	p_{SO_2}	y_{SO_2}	C_{SO_2}	p_{SO_2}
ppmv	mg·L^{-1}	Pa	ppmv	mg·L^{-1}	Pa
24.11	15.29	3.43	514.88	132.15	73.14
41.18	17.58	5.79	531.41	144.67	75.47
62.63	21.55	8.86	561.71	157.20	79.32
113.99	41.03	16.22	623.91	182.24	88.26
169.50	52.16	24.06	657.71	198.94	93.57
192.71	54.95	27.40	688.98	228.16	97.70
241.40	64.68	34.28	728.03	236.50	103.08
304.48	83.47	43.28	738.73	244.85	104.51
353.57	90.42	50.25	763.29	279.64	108.19
397.29	100.16	56.06	809.36	310.25	114.39
448.15	115.47	63.93	842.40	338.07	119.42
512.05	134.25	72.97	861.59	375.64	122.16

Table 8. GLE Data for the SO_2 + N_2 + EG System at 303.15 K and 101.86 kPa

y_{SO_2}	C_{SO_2}	p_{SO_2}	y_{SO_2}	C_{SO_2}	p_{SO_2}
ppmv	mg·L^{-1}	Pa	ppmv	mg·L^{-1}	Pa
58.30	27.56	5.94	579.11	128.70	58.80
128.52	32.76	13.18	625.06	140.84	63.76
167.66	35.65	17.08	746.44	155.28	76.04
229.15	49.52	23.41	779.99	170.89	79.46
340.15	64.55	34.57	787.62	171.47	80.08
341.37	63.97	34.59	802.74	182.27	81.61
410.99	87.09	42.02	865.02	196.14	88.12
445.27	92.87	45.35	902.44	216.94	92.00
483.53	102.12	49.45	941.71	242.37	96.01
519.42	107.89	53.29	984.14	251.62	100.23
561.66	124.65	57.21			

Table 9. GLE Data for the SO_2 + N_2 + EG System at 303.15 K and 112.53 kPa

y_{SO_2}	C_{SO_2}	p_{SO_2}	y_{SO_2}	C_{SO_2}	p_{SO_2}
ppmv	mg·L^{-1}	Pa	ppmv	mg·L^{-1}	Pa
63.71	68.23	7.16	564.87	112.48	63.61
120.96	36.20	13.68	611.12	130.40	68.76
153.00	39.66	17.16	674.01	142.53	75.77
235.26	51.80	26.46	691.09	157.93	77.89
265.94	57.00	29.83	733.83	161.03	82.59
287.40	62.20	32.31	795.38	184.51	89.50
310.01	66.83	34.85	847.22	200.69	95.11
396.71	85.90	44.78	871.73	207.63	97.89
460.07	92.83	51.71	922.71	235.37	103.61
525.14	105.55	59.04	951.31	258.48	106.84
562.74	117.11	63.17			

Table 10. GLE Data for the SO_2 + N_2 + EG System at 303.15 K and 123.19 kPa

y_{SO_2}	C_{SO_2}	p_{SO_2}	y_{SO_2}	C_{SO_2}	p_{SO_2}
ppmv	mg·L^{-1}	Pa	ppmv	mg·L^{-1}	Pa
69.41	34.69	8.52	567.17	126.02	69.37
104.17	40.47	12.74	597.98	127.17	73.40
119.33	46.25	14.61	609.16	128.33	74.558
173.04	52.61	21.22	651.60	145.67	80.11
220.80	64.17	27.11	705.23	164.16	86.68
292.66	79.79	35.88	730.30	166.47	89.02
296.28	81.50	36.20	794.89	190.75	97.18
343.84	92.50	42.01	833.82	208.08	101.90
436.89	101.73	53.57	880.86	211.55	107.74
542.58	116.77	66.44	901.37	233.51	110.25

Table 11. GLE Data for the SO_2 + N_2 + EG System at 303.15 K and 133.85 kPa

y_{SO_2}	C_{SO_2}	p_{SO_2}	y_{SO_2}	C_{SO_2}	p_{SO_2}
ppmv	mg·L^{-1}	Pa	ppmv	mg·L^{-1}	Pa
44.62	15.02	5.88	631.18	108.63	83.10
101.32	20.80	13.35	638.26	109.79	84.17
153.53	30.04	20.17	700.71	128.28	92.43
245.86	46.80	32.65	778.13	151.40	103.00
277.75	41.59	36.72	796.03	172.20	105.00
340.13	53.15	44.99	873.13	206.88	115.48
405.43	69.33	53.46	882.28	210.35	116.69
456.06	80.89	60.04	913.57	230.00	120.87
553.58	100.54	73.08	926.62	251.96	122.62
593.07	91.29	78.22			

(Hebei province, China) with the accuracy of ± 0.133 kPa, using SO_2 + N_2 mixtures (1970 ppmv) in the SO_2 partial pressure range from (0 to 120) Pa. First, 300 mL of EG solution was poured into the jacketed vessel (1) as the absorption solution. Then, about 3000 mL of the SO_2 + N_2 mixture gas was poured into the experimental system and recycled by the gas recycle pump (4): the temperature and pressure in the experimental system are set at the experimental condition. Meanwhile, the EG extracts SO_2 from the SO_2 + N_2 mixture gas to reach the GLE situation, and at this time, the concentrations of SO_2 separately in the gas phase and in the liquid phase can be determined as the GLE data. We repeated the above performance with different SO_2 + N_2 mixture gases, and the different GLE data were obtained.

The concentrations of SO_2 in the gas phase were determined by a gas chromatograph on a 2 × 1/8 (m × inch) Porapak Q packed column using an Agilent 6890N gas chromatograph (GC) and an FPD detector linked to an HP6890 workstation. The carrier gas was nitrogen (flow rate 30 mL·min^{-1}); the oven temperature was designed at 393.15 K; and the proportional loop was chosen for a volume of 5 μL. In all cases, the injections were repeated at least seven times, and the average results were reported. To calibrate the GC FPD detector, the external standard method was used.

Table 12. GLE Data for the SO$_2$ + N$_2$ + EG System at 303.15 K and 144.53 kPa

y_{SO_2}	C_{SO_2}	p_{SO_2}	y_{SO_2}	C_{SO_2}	p_{SO_2}
ppmv	mg·L^{-1}	Pa	ppmv	mg·L^{-1}	Pa
58.90	28.53	8.30	552.10	107.13	78.32
61.80	21.60	8.75	589.48	117.53	83.79
115.75	32.00	16.31	645.67	134.87	91.78
193.79	41.25	27.37	689.29	161.45	97.98
287.08	56.27	40.72	714.62	182.26	101.58
345.20	72.45	49.02	760.82	192.66	106.93
355.61	71.30	49.97	805.74	213.47	113.50
443.51	85.17	62.95	845.50	241.21	119.10
468.74	94.42	66.50	853.35	250.45	120.48
492.14	99.04	69.83			

Table 13. GLE Data for the SO$_2$ + N$_2$ + EG System at 308.15 K and 101.86 kPa

y_{SO_2}	C_{SO_2}	p_{SO_2}	y_{SO_2}	C_{SO_2}	p_{SO_2}
ppmv	mg·L^{-1}	Pa	ppmv	mg·L^{-1}	Pa
19.73	18.03	2.02	587.88	93.07	60.06
88.13	41.62	9.00	603.24	101.65	61.59
173.80	52.87	17.75	673.67	111.83	68.98
193.36	53.94	19.69	753.50	125.77	77.14
236.55	63.59	24.15	817.46	140.78	83.65
275.89	60.91	28.18	844.02	152.03	86.55
323.54	66.81	33.05	864.77	157.93	88.04
396.24	74.85	40.48	901.51	169.18	92.20
451.70	82.89	46.01	935.27	194.38	95.42
481.18	84.50	49.15	952.73	195.98	97.43
534.88	87.18	54.63	980.60	200.81	99.82

Table 14. GLE Data for the SO$_2$ + N$_2$ + EG System at 308.15 K and 112.53 kPa

y_{SO_2}	C_{SO_2}	p_{SO_2}	y_{SO_2}	C_{SO_2}	p_{SO_2}
ppmv	mg·L^{-1}	Pa	ppmv	mg·L^{-1}	Pa
34.66	31.99	3.89	663.91	130.62	74.74
80.90	33.06	9.09	687.83	139.73	77.31
145.10	37.89	16.31	734.51	157.42	82.57
182.12	46.46	20.50	762.67	166.90	85.53
209.19	49.14	23.48	780.86	205.49	87.59
236.32	60.40	26.55	812.73	199.06	91.11
327.17	77.55	36.82	847.25	206.56	95.04
386.74	90.95	43.31	889.90	225.86	100.03
453.34	102.21	50.96	918.65	243.01	102.82
515.39	109.18	57.96	938.17	253.73	105.13
534.88	116.14	60.18	970.60	275.17	108.79
610.84	124.18	68.70			

Table 15. GLE Data for the SO$_2$ + N$_2$ + EG System at 308.15 K and 123.19 kPa

y_{SO_2}	C_{SO_2}	p_{SO_2}	y_{SO_2}	C_{SO_2}	p_{SO_2}
ppmv	mg·L^{-1}	Pa	ppmv	mg·L^{-1}	Pa
17.80	21.06	2.18	545.14	120.17	66.47
26.45	23.66	3.22	572.61	130.58	69.94
45.85	34.07	5.59	591.13	131.62	72.08
106.32	51.76	12.96	629.76	156.60	76.87
194.23	56.44	23.72	683.89	165.96	83.35
240.53	73.09	29.51	695.58	181.57	85.07
253.07	67.89	30.85	733.67	203.42	89.71
319.69	78.82	38.96	772.65	219.03	94.52
376.48	84.79	45.89	803.38	236.72	98.13
423.58	100.40	51.79	831.00	257.54	101.39
465.86	117.05	56.90	855.48	279.39	104.49
481.25	119.13	58.67			

Table 16. GLE Data for the SO$_2$ + N$_2$ + EG System at 308.15 K and 133.85 kPa

y_{SO_2}	C_{SO_2}	p_{SO_2}	y_{SO_2}	C_{SO_2}	p_{SO_2}
ppmv	mg·L^{-1}	Pa	ppmv	mg·L^{-1}	Pa
18.53	6.493	2.42	558.33	127.73	73.66
22.86	10.66	3.01	566.78	130.85	74.58
47.59	13.26	6.21	637.68	145.15	83.49
80.43	23.66	10.48	661.85	162.84	87.32
85.65	23.14	11.30	697.43	185.73	92.01
119.03	33.03	15.70	710.61	194.06	93.96
168.73	44.48	22.25	736.42	205.51	97.16
217.23	57.48	28.50	762.99	216.95	100.68
272.34	68.41	35.88	773.84	248.17	101.70
342.99	80.90	45.16	803.35	268.98	105.54
346.77	76.74	45.58	820.60	267.94	108.34
398.94	87.66	52.38	836.79	278.35	110.21
441.24	97.03	58.07	863.78	288.76	114.00
500.22	123.57	65.98	872.76	291.88	114.70
504.22	109.00	66.44	881.58	298.12	116.11

Table 17. GLE Data for the SO$_2$ + N$_2$ + EG System at 308.15 K and 144.53 kPa

y_{SO_2}	C_{SO_2}	p_{SO_2}	y_{SO_2}	C_{SO_2}	p_{SO_2}
ppmv	mg·L^{-1}	Pa	ppmv	mg·L^{-1}	Pa
13.60	5.45	1.93	447.67	128.50	63.40
33.53	13.26	4.76	481.49	137.86	67.98
65.29	41.36	9.25	516.35	159.72	73.02
90.99	31.99	12.90	535.88	168.04	75.66
118.26	45.52	16.81	562.72	187.81	79.44
153.82	49.68	21.72	579.84	205.51	82.16
158.75	50.72	22.54	721.82	225.28	101.93
201.68	59.57	28.70	721.82	246.09	101.99
251.31	73.09	35.69	758.85	252.33	107.44
260.35	76.22	36.84	759.74	258.58	107.98
308.92	90.79	43.62	787.49	275.23	111.67
351.32	99.11	49.70	803.16	295.00	114.43
389.61	109.52	55.28	823.69	307.49	117.19
408.89	113.93	57.91	835.33	324.14	118.62

Table 18. GLE Data for the SO$_2$ + N$_2$ + EG System at 313.15 K and 101.86 kPa

y_{SO_2}	C_{SO_2}	p_{SO_2}	y_{SO_2}	C_{SO_2}	p_{SO_2}
ppmv	mg·L^{-1}	Pa	ppmv	mg·L^{-1}	Pa
9.01	4.69	0.92	595.06	145.71	60.77
65.64	21.87	6.69	624.07	135.31	63.57
120.27	32.27	12.29	624.79	139.47	63.67
148.28	37.99	15.14	672.32	149.88	68.67
169.80	39.56	17.39	689.12	151.96	70.00
203.76	47.36	20.76	694.70	158.20	71.12
239.95	54.12	24.48	710.78	159.24	72.29
297.52	64.53	30.31	758.53	176.93	77.27
302.20	74.94	30.79	803.16	210.23	81.81
361.26	80.14	36.81	824.51	197.74	83.99
418.59	88.99	42.75	840.53	223.76	85.85
446.37	108.25	45.52	867.21	238.33	88.31
476.66	98.35	48.56	889.17	251.86	90.58
502.88	115.53	51.23	892.36	254.98	90.90
562.47	125.94	57.43	914.54	267.47	93.16

The sulfur(IV) concentration in the liquid phase (C_{SO_2}, mg·L^{-1}) was determined, once equilibrium was reached, by adding a known volume of solution from the vessel to a known volume of standard iodine solution. The excess iodine solution was back-titrated with the standard sodium thiosulfate solution.[10] The overall uncertainty in the determination of the sulfur(IV) concentration was estimated to be ± 0.6 %.

Results and Discussions

The GC FPD detector was calibrated with the standard SO$_2$ + N$_2$ mixture gases, and the calibrated results are shown in Table 1.

Table 1 shows that GC method presented high stability in the analytical processes of SO$_2$ concentration, so that the method can be used in following GLE studies.

The calibration curves for the FPD detector were established by running the standard gas mixtures presented in the equipment through the GC at various temperaments and pressures. The calibration relation is calculated by the double logarithm method and shown in Table 2.

Table 19. GLE Data for the SO_2 + N_2 + EG System at 313.15 K and 112.53 kPa

y_{SO_2}	C_{SO_2}	p_{SO_2}	y_{SO_2}	C_{SO_2}	p_{SO_2}
ppmv	mg·L^{-1}	Pa	ppmv	mg·L^{-1}	Pa
24.09	14.29	2.70	407.21	84.83	45.70
19.81	12.56	2.22	458.87	94.02	51.46
45.95	14.29	5.14	508.13	111.24	57.02
46.67	13.71	5.22	572.85	119.28	64.22
91.99	29.79	10.32	619.39	128.46	69.53
110.59	30.94	12.37	666.56	160.61	74.79
59.18	19.45	6.63	712.35	184.72	79.74
135.89	37.25	15.24	759.40	201.95	84.95
197.93	46.44	22.22	793.35	223.76	88.94
272.24	55.62	30.49	810.12	227.21	90.81
269.41	56.77	30.23	837.47	253.61	93.79
313.25	60.79	35.11	862.52	266.24	96.40
328.67	71.06	36.81			

Table 20. GLE Data for the SO_2 + N_2 + EG System at 313.15 K and 123.19 kPa

y_{SO_2}	C_{SO_2}	p_{SO_2}	y_{SO_2}	C_{SO_2}	p_{SO_2}
ppmv	mg·L^{-1}	Pa	ppmv	mg·L^{-1}	Pa
17.89	8.51	2.20	632.97	154.33	77.50
96.82	25.73	11.86	670.48	160.64	82.16
118.27	33.77	14.50	684.62	168.68	83.91
122.22	35.49	14.98	708.00	189.92	86.75
140.45	37.22	17.20	726.30	175.47	89.00
209.70	51.00	25.67	747.15	203.03	91.65
213.10	59.03	26.10	753.82	217.95	92.47
346.37	86.01	42.42	791.89	242.06	96.98
396.13	88.31	48.59	814.25	253.55	99.85
496.24	103.24	60.77	815.96	268.47	100.12
525.42	118.16	64.35	839.97	276.51	102.98
561.08	123.33	68.72	847.83	281.10	103.99
616.76	145.14	75.52	850.33	283.40	104.28

Table 21. GLE Data for the SO_2 + N_2 + EG System at 313.15 K and 133.85 kPa

y_{SO_2}	C_{SO_2}	p_{SO_2}	y_{SO_2}	C_{SO_2}	p_{SO_2}
ppmv	mg·L^{-1}	Pa	ppmv	mg·L^{-1}	Pa
4.16	18.80	0.55	403.44	120.02	53.63
22.29	20.01	2.96	472.86	136.99	62.48
64.66	30.31	8.61	499.72	145.48	66.09
78.83	33.95	10.50	508.46	156.39	67.68
89.20	38.19	11.88	549.85	170.93	73.10
98.11	40.01	13.01	575.08	180.63	76.36
118.40	42.44	15.74	602.25	200.03	80.06
164.41	52.74	21.84	637.70	212.15	84.95
217.75	61.22	28.95	675.73	241.24	90.07
192.70	75.17	25.62	698.60	265.48	92.68
235.44	78.81	31.22	733.50	290.94	97.51
279.22	95.78	37.18	753.95	299.42	100.23
326.74	103.05	43.44			

Table 22. GLE Data for the SO_2 + N_2 + EG System at 313.15 K and 144.53 kPa

y_{SO_2}	C_{SO_2}	p_{SO_2}	y_{SO_2}	C_{SO_2}	p_{SO_2}
ppmv	mg·L^{-1}	Pa	ppmv	mg·L^{-1}	Pa
6.07	16.55	0.87	376.91	111.27	54.00
15.15	22.29	2.14	436.27	126.20	62.50
26.30	22.86	3.73	482.76	144.57	69.26
62.30	29.18	8.95	514.65	154.90	73.81
41.18	22.29	5.91	552.70	181.88	79.30
42.99	23.44	6.17	566.56	188.10	81.16
61.13	30.33	8.79	596.03	216.80	85.46
71.76	39.51	10.18	617.02	222.55	88.34
92.31	36.64	13.20	656.77	240.92	94.23
117.17	45.25	16.77	673.25	258.14	96.40
151.78	56.74	21.74	689.72	274.21	98.61
161.35	58.46	23.08	708.22	279.95	101.62
199.04	69.36	28.40	729.23	284.55	104.65
234.68	80.85	33.64	747.04	312.10	107.06
327.91	100.37	47.08	757.71	323.58	108.71
413.68	119.31	59.35			

The maximum deviation value is defined as

$$y' = \max((y_{max} - \bar{y}), (\bar{y} - y_{min})) \qquad (2)$$

where y_{max}, y_{min}, and $\bar{y}$ (y_{SO_2}) are, respectively, calculated by formula eqs 3 to 5 as follows

Figure 2. GLE curves for the SO_2 + N_2 + EG system at 298.15 K and various pressures: □, 101.86 kPa; ○, 112.50 kPa; Δ, 123.19 kPa; +, 133.53 kPa; ×, 144.53 kPa.

Figure 3. GLE curves for the SO_2 + N_2 + EG system at 303.15 K and various pressures: □, 101.86 kPa; ○, 112.50 kPa; Δ, 123.19 kPa; +, 133.53 kPa; ×, 144.53 kPa.

In Table 2, *x* represents the logarithm of the SO_2 peak area and *y* represents the logarithm of the volume concentration of SO_2 in the gas phase. Meanwhile, R^2 is above 0.99 under setting conditions.

In this work, isothermal GLE data for the SO_2 + N_2 mixture gas with EG was determined in the temperature range from (298.15 to 313.15) K with the step of 5 K and the SO_2 partial pressure in the gas phase up to 120 Pa. The experimental SO_2 concentration y_{exptl} is acquired by

$$y_{exptl} = \frac{p - p_1}{p_2 - p_1} y_2' + \frac{p_2 - p}{p_2 - p_1} y_1' \qquad (1)$$

where p, p_1, and p_2 represent, respectively, the system total pressure, low calibration pressure, and high calibration pressure, $p_2 \geq p \geq p_1$.
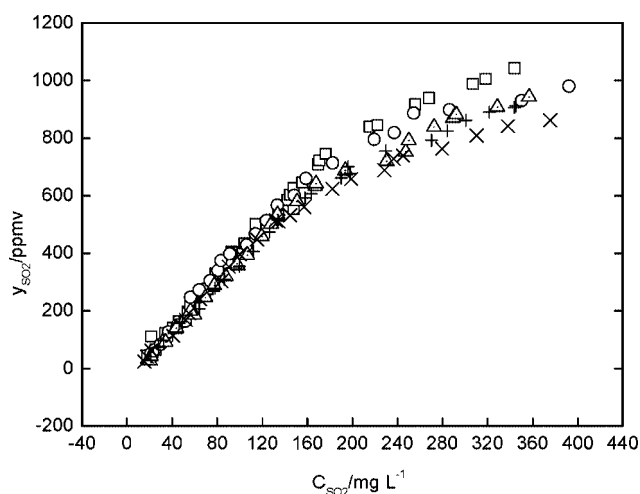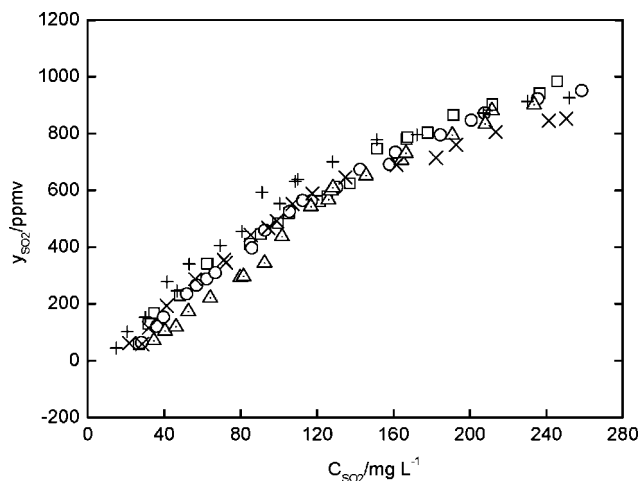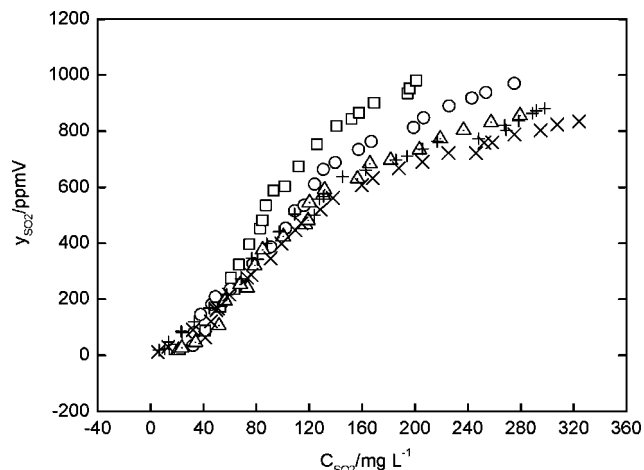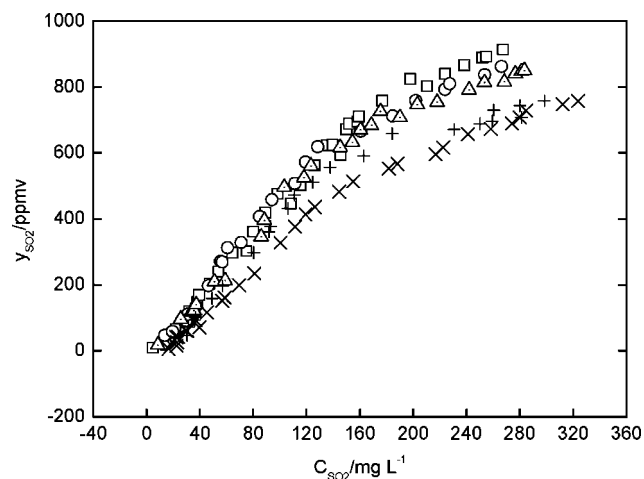
Figure 4. GLE curves for the SO_2 + N_2 + EG system at 308.15 K and various pressures: □, 101.86 kPa; ○, 112.50 kPa; Δ, 123.19 kPa; +, 133.53 kPa; ×, 144.53 kPa.

Figure 5. GLE curves for the SO_2 + N_2 + EG system at 313.15 K and various pressures: □, 101.86 kPa; ○, 112.50 kPa; Δ, 123.19 kPa; +, 133.53 kPa; ×, 144.53 kPa.
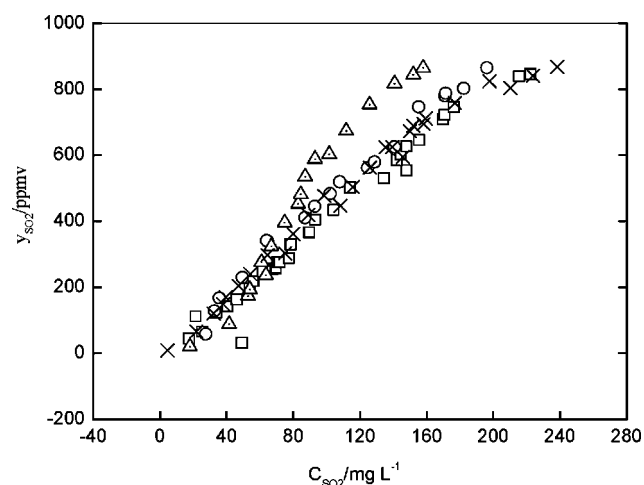
Figure 6. GLE curves for the SO_2 + N_2 + EG system at 101.86 kPa and various temperatures: □, 298.15 K; ○, 303.15 K; Δ, 308.15 K; ×, 313.15 K.

$$y_{max} = \max(y_{1,exptl}, y_{2,exptl}, y_{3,exptl}, \ldots, y_{7,exptl}) \quad (3)$$

$$y_{min} = \min(y_{1,exptl}, y_{2,exptl}, y_{3,exptl}, \ldots, y_{7,exptl}) \quad (4)$$
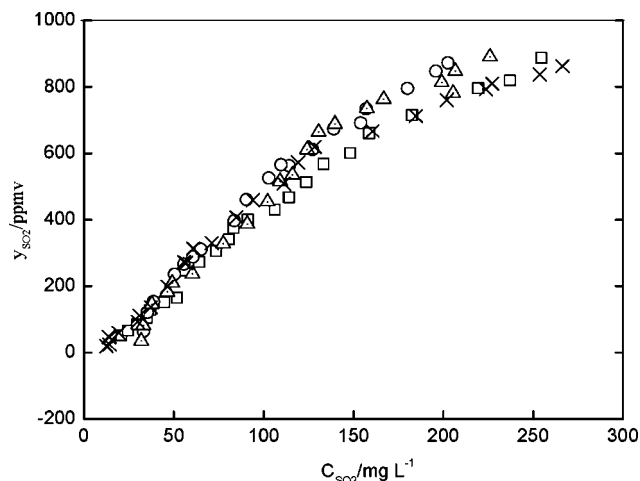
Figure 7. GLE curves for the SO_2 + N_2 + EG system at 112.53 kPa and various temperatures: □, 298.15 K; ○, 303.15 K; Δ, 308.15 K; ×, 313.15 K.
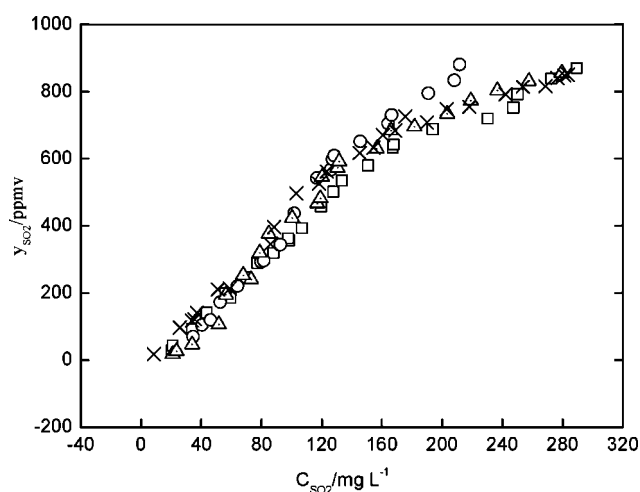
Figure 8. GLE curves for the SO_2 + N_2 + EG system at 123.19 kPa and various temperatures: □, 298.15 K; ○, 303.15 K; Δ, 308.15 K; ×, 313.15 K.

$$\bar{y} = \sum_{i=1}^{7} y_{i,exptl}/7 \quad (5)$$

The maximum relative error is acquired by

$$\delta = y'/\bar{y} \cdot 100 \% \quad (6)$$

The partial pressure of SO_2 (p_{SO_2}) in the gas phase is given by

$$p_{SO_2} = p \cdot \bar{y} \quad (7)$$

The GLE data for the SO_2 + N_2 + EG system, respectively, at (298.15, 303.15, 308.15, and 313.15) K and the total pressures of (101.86, 112.53, 123.19, 133.85, and 144.53) kPa are shown in Tables 3 to and Figures 2 to 5.

Figures 2 to 5 show that the solubility of SO_2 in EG is increased with increasing pressure at constant temperature. Figures 6 to 10 show that the solubility of SO_2 in EG is decreased with increasing temperature under constant pressure.

Figures 6 to 10 display that the solubility of SO_2 in EG displayed obvious temperature dependence. Especially, Figures 9 and 10 show that EG displays stronger solubility to SO_2 at 313 K and higher total pressures.

Conclusion

In this paper, the GLE data for the system of SO_2 + N_2 + EG were determined, respectively, at (298.15, 303.15, 308.15,

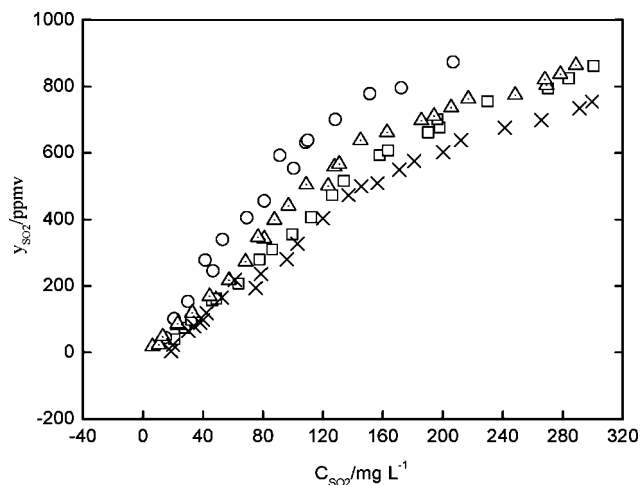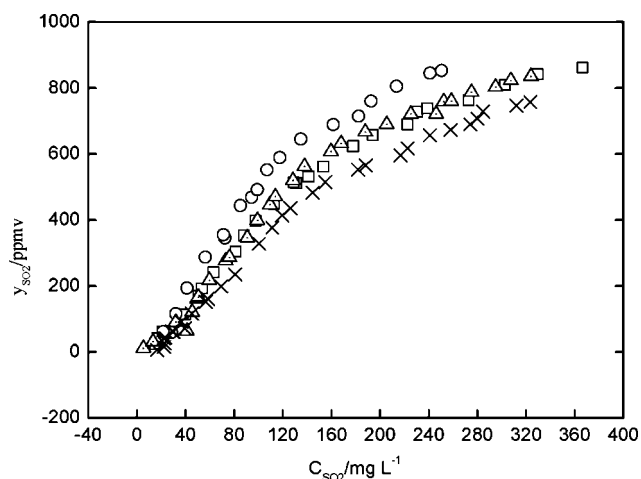**Figure 9.** GLE curves for the $SO_2 + N_2 + EG$ system at 133.85 kPa and various temperatures: □, 298.15 K; ○, 303.15 K; △, 308.15 K; ×, 313.15 K.

Figure 10. GLE curves for the $SO_2 + N_2 + EG$ system at 144.53 kPa and various temperatures: □, 298.15 K; ○, 303.15 K; △, 308.15 K; ×, 313.15 K.

and 313.15) K and the SO_2 partial pressures in the range from (0 to 120) Pa, with the uncertainties within ± 0.02 K for temperature, ± 0.133 kPa for the total pressure, ± 2.5 % for the SO_2 concentration in the gas phase, and ± 0.6 % for the SO_2 concentration in the liquid phase.

Literature Cited

(1) Siddiqi, M. A.; Krissmann, J.; Peters-Gerth, P.; Luckas, M.; Lucas, K. Spectrophotometric Measurement of the Vapour-Liquid Equilibria of (Sulphur Dioxide + Water). *J. Chem. Thermodyn.* **1996**, *28*, 685–700.
(2) Esteve, X.; Conesa, A.; Coronas, A. Liquid Densities, Kinematic Viscosities, and Heat Capacities of Some Alkylene Glycol Dialkyl Ethers. *J. Chem. Eng. Data* **2003**, *48*, 392–397.
(3) Ku, H. C.; Tu, C. H. Densities and Viscosities of Seven Glycol Ethers from 299.15 to 343.15 K. *J. Chem. Eng. Data* **2000**, *45*, 391–394.
(4) Valtz, A.; Coquelet, C.; Richon, D. Vapor-Liquid Equilibrium Data for the Sulfur Dioxide (SO_2) + 1,1,1,2,3,3,3-heptafluoropropane (R227ea) System at Temperatures from 288.07 to 403.19 K and Pressures up to 5.38 MPa. Representation of the Critical Point and Azeotrope Temperature Dependence. *Fluid Phase Equilib.* **2004**, *220*, 77–83.
(5) Nagel, D.; Kermadec, R. D.; Lintz, H. G.; Roizard, C.; Lapicque, F. Absorption of Sulfur Dioxide in N-formylmorpholine: Investigations of the Kinetics of the Liquid Phase Reaction. *Chem. Eng. Sci.* **2002**, *57*, 4883–4893.
(6) De Kermadec, R.; Lapicque, F.; Roizard, D.; Roizard, C. Characterization of the SO_2-N-formylmorpholine Complex: Application to A Regenerative Process for Waste Gas Scrubbing. *Ind. Eng. Chem. Res.* **2002**, *41*, 153–163.
(7) Schubert, C. N.; Echter, W. I. The Method of Polymer Ethylene Glycol for Removal Pollution from Gases. CN. Patent. 1364096A, 2002.
(8) Li, X. X.; Liu, Y. X.; Wei, X. H. Hydrolysis of Carbonyl Sulfide in Binary Mixture of Diethylene Glycol Diethyl Ether with Water. *Chin. J. Chem. Eng.* **2005**, *13* (2), 234–238.
(9) Wei, X. H. Desulfurication & Decarburization Solution Activities. CN. Patent.02130605. 2, 2002.
(10) Rodriguez-Sevilla, J.; Alvarez, M.; Liminana, G.; Diaz, M. C. Dilute SO_2 Absorption Equilibria in Aqueous HCl and NaCl Solutions at 298.15 K. *J. Chem. Eng. Data* **2002**, *47*, 1339–1345.